

Phonon softening and anomalous mode near the $x_c=0.5$ quantum critical point in $\text{Ca}_{2-x}\text{Sr}_x\text{RuO}_4$ R. G. Moore,^{1,*} M. D. Lumsden,² M. B. Stone,² Jiandi Zhang,³ Y. Chen,⁴ J. W. Lynn,⁴ R. Jin,^{5,1} D. Mandrus,^{5,1} and E. W. Plummer¹¹Department of Physics and Astronomy, The University of Tennessee, Knoxville, Tennessee 37996, USA²Neutron Scattering Sciences Division, Oak Ridge National Laboratory, Oak Ridge, Tennessee 32831, USA³Department of Physics, Florida International University, Miami, Florida 33199, USA⁴NIST Center for Neutron Research, National Institute of Standards and Technology, Gaithersburg, Maryland 20899, USA⁵Materials Science and Technology Division, Oak Ridge National Laboratory, Oak Ridge, Tennessee 37831, USA

(Received 14 April 2009; published 4 May 2009)

Inelastic neutron scattering is used to measure the temperature-dependent phonon dispersion in $\text{Ca}_{2-x}\text{Sr}_x\text{RuO}_4$ ($x=0.4, 0.6$). The in-plane Σ_4 octahedral tilt mode softens significantly at the zone boundary of the high-temperature tetragonal (HTT) $I4_1/acd$ structure as the temperature approaches the transition to a low-temperature orthorhombic (LTO) $Pbca$ phase. This behavior is similar to that in La_2CuO_4 , but an inelastic feature that is not found in the cuprate is present. An anomalous phonon mode is observed at energy transfers greater than the Σ_4 , albeit with similar dispersion. This anomalous phonon mode never softens below ~ 5 meV, even for temperatures below the HTT-LTO transition. This mode is attributed to the presence of intrinsic structural disorder within the $I4_1/acd$ tetragonal structure of the doped ruthenate.

DOI: 10.1103/PhysRevB.79.172301

PACS number(s): 63.20.dd, 61.05.fg, 63.50.-x, 64.70.K-

The discovery of exotic superconductivity in Sr_2RuO_4 and its structural similarity to La_2CuO_4 has generated much interest in the $\text{Ca}_{2-x}\text{Sr}_x\text{RuO}_4$ (CSRO) family of compounds.¹⁻⁵ Their physical properties as a function of doping have remarkable similarities with those of the high-temperature superconductor $\text{La}_{2-x}\text{Sr}_x\text{CuO}_4$ (LSCO).⁶ Nevertheless, it is important to realize that Sr and Ca are isoelectronic, such that Ca substitution does not change the valence electron number, i.e., does not change the band filling, in contrast with Sr doping of the cuprate.^{3,4,6,7} In addition to providing a new system where the evolution from antiferromagnetism to superconductivity can be explored, the phase diagram of the single-layered Ruddlesden-Popper CSRO compounds contains rich and exotic behavior attributed to numerous nearly degenerate structural and magnetic instabilities. For instance, for $x < 0.2$, an antiferromagnetic (AFM) insulating ground state and metal-insulator phase transitions are observed,³⁻⁵ while a metamagnetic transition is observed for $x \sim 0.2$ accompanied by anisotropic thermal-expansion anomalies that can be reversed in a magnetic field.^{3,8} For $0.2 \leq x < 0.5$, short-range AFM correlations exist but vanish at $x_c \approx 0.5$, where the spin susceptibility is critically enhanced, indicating a ferromagnetic instability point.^{3,4,7} This critical concentration, $x_c \approx 0.5$, is also the $T=0$ K terminus *quantum critical point* (QCP) for the line of structural phase transitions between the high-temperature tetragonal (HTT) and low-temperature orthorhombic (LTO) phases.^{3,4}

Inelastic-neutron-scattering (INS) measurements of the temperature dependence of the Σ_4 phonon mode in $\text{Ca}_{2-x}\text{Sr}_x\text{RuO}_4$ ($x=0.4, 0.6$) were performed. These concentrations are in immediate proximity to the QCP while allowing investigation of mode softening both with and without traversing the HTT-LTO phase boundary. This choice of concentrations is also motivated by interest in surface phases and phase transitions in CSRO, and the possibility of resolving questions concerning surface mechanisms by understanding the bulk phonon behavior.⁹

Figure 1 summarizes the three structural phases of the

CSRO compounds for $x \leq 0.5$. Generically, the structure consists of Ru sites in an octahedral coordination with neighboring O sites. The octahedra form a layered structure in the ab plane with neighboring planes along the c axis separated by Ca/Sr layers. The structural phase transitions are associated with changes in the octahedral tilt and rotation as well as the octahedral stacking sequence along the c axis. While both $x=0.4$ and $x=0.6$ start in the HTT $I4_1/acd$ symmetry at room temperature, $x=0.4$ enters into a LTO $Pbca$ symmetry upon

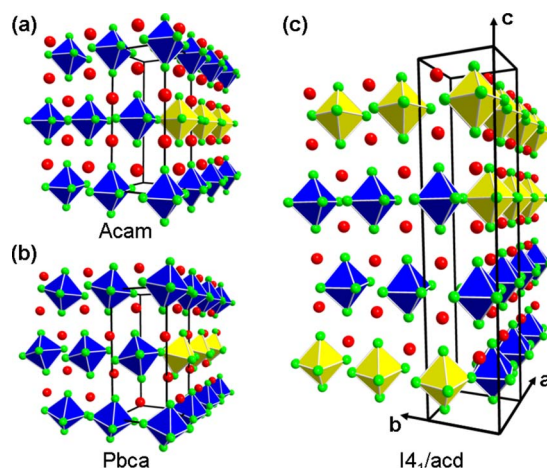


FIG. 1. (Color online) Structural phases of the CSRO family for $x \leq 1.5$. RuO_6 octahedra are illustrated with yellow (blue) octahedra representing clockwise (counterclockwise) rotation relative to the c axis. Oxygen (Ca/Sr) sites are represented by green (red) spheres and unit cells are shown as black lines. Only octahedra along the $[100]$ and $[010]$ faces are shown for clarity. CSRO $x \leq 0.2$ presents the (a) $Acam$ symmetry at high temperatures and (b) $Pbca$ symmetry at low temperatures. Both $x=0.4$ and $x=0.6$ present the (c) $I4_1/acd$ symmetry at high temperatures but the LTO phase of $x=0.4$ involves a structural frustration between the preferred RuO_6 rotation stacking periodicity of the $I4_1/acd$ phase and the induced tilt periodicity of the $Pbca$ phase (Refs. 4 and 10).

cooling.^{3,4,10} While the LTO phase is created by a static tilt of the RuO_6 , structural frustration is introduced due to the preferred stacking periodicities along the c axis observed for x away from the QCP.¹⁰ The Σ_4 transverse-acoustic phonon mode is related to the tilt of the layered Ru octahedra and, as such, is particularly sensitive to their distortions in different portions of the CSRO phase diagram.

Single-crystal samples were grown using the floating-zone technique, $m_{x=0.4} \approx 3$ g and $m_{x=0.6} \approx 4$ g. INS measurements for $x=0.4$ were performed using the HB1 triple-axis spectrometer (TAS) at the High Flux Isotope Reactor (HFIR) at ORNL and the BT-7 TAS at the NIST Center for Neutron Research. INS measurements for $x=0.6$ were performed using the HB3 TAS at HFIR. The HB1 and HB3 instrument configurations consisted of a fixed-focus PG(002) monochromator and a flat PG(002) analyzer with collimations of $48'-40'-40'-240'$. The BT-7 configuration consisted of a variable-focus PG(002) monochromator and a focusing PG(002) analyzer with collimations of open- $50'-40'$ -open. All measurements employed a fixed final neutron energy of 14.7 meV with a pyrolytic graphite (PG) filter in the scattered beam. Samples were mounted in the (hhl) scattering plane and indexed in the $I4/mmm$ symmetry of pure Sr_2RuO_4 . Unless noted, all (hkl) coordinates refer to this notation. The $(1.5\ 1.5\ 2)$ wave vector is a zone boundary for both the $I4/mmm$ and $I4_1/acd$ symmetries. However, due to the static RuO_6 rotation, a glide plane symmetry is established and the $(1.5\ 1.5\ 2)$ Bragg peak is extinguished for $T > T_C$. As one cools through the HTT-LTO transition, the ensuing static distortion results in the appearance of this Bragg peak as this wave vector becomes a zone center for the orthorhombic $Pbca$ phase. Using the Bragg peak intensity as an order parameter, we find $T_C \sim 155$ K for the $x=0.4$ sample, consistent with prior studies.^{3,4} No hysteresis for the order parameter is observed, consistent with the expected second-order phase transition.

Constant wave-vector scans were performed to determine the temperature-dependent dispersion of the Σ_4 phonon mode. This phonon propagates in the $[1\ 1\ 0]$ direction, but the motion of the oxygen atoms due to the static rotation results in mixed longitudinal and transverse components. Regions near the $(1.5\ 1.5\ 2)$ and $(0.5\ 0.5\ 6)$ wave vectors provided clean Σ_4 phonon measurements because of structure factor considerations similar to those of La_2CuO_4 and Sr_2RuO_4 .^{11,12}

Phonon-dispersion curves were found by comparing individual constant wave-vector scans to multiple Gaussian peaks. A Gaussian peak was assumed for the incoherent peak plus one for each mode observed. All data were corrected for monitor contamination due to higher-order Bragg scattering from the PG(002) monochromator. Data collected with a fixed-focus monochromator were corrected to account for deviations in beam size as a function of incident energy. To improve the comparison and allow all fit parameters to be unrestricted during analysis, the data were first smoothed using wavelet shrinkage.^{13,14} Figure 2 shows constant- Q scans, corrected as described above, at the $(1.5\ 1.5\ 2)$ Brillouin-zone boundary for $x=0.4$ and $x=0.6$.

The scans shown in Fig. 2 reveal several spectral features with the lowest-energy feature being the Σ_4 mode. In addition,

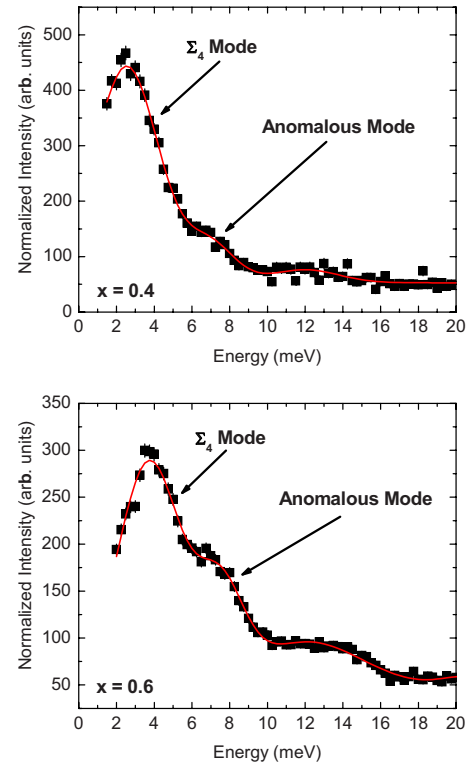


FIG. 2. (Color online) Zone-boundary $(1.5\ 1.5\ 2)$ INS data for $x=0.4$ at $T=270$ K and $x=0.6$ at $T=200$ K. The Σ_4 and anomalous modes are annotated and observed in all scans. Red line is the result from multiple Gaussian fits. Uncertainties where indicated are statistical and represent one standard deviation.

tion, a slightly higher-energy phonon mode is observed in both samples. This mode appears in all Brillouin zones where the Σ_4 mode is present and possesses an intensity and wave-vector modulation which mimics the Σ_4 mode. This anomalous mode is not expected from normal-mode analysis^{10,12} and, as such, it is anomalous in nature. The fundamental reasons for the existence of this anomalous mode must be explored to fully understand the physics of the system. In addition to these two modes, a higher-energy lattice excitation is also seen in Fig. 2 that is not examined here.

Constant- Q scans near $(1.5\ 1.5\ 2)$ and $(0\ 0\ 6)$ are combined to form the dispersion curves shown in Fig. 3. This dispersion is plotted in the $I4/mmm$ notation to allow comparison with similar soft-mode behavior in La_2CuO_4 .¹¹ The anomalous mode is clearly visible in Fig. 3 with a dispersion that mimics the Σ_4 mode displaced in energy. This is in contrast to La_2CuO_4 , where only the single Σ_4 mode is observed. The Σ_4 phonon mode is doubly degenerate with two possible tilt modes around $[0\bar{1}0]$ and $[100]$. The simplest explanation for the presence of two modes would be a lifting of this degeneracy. However, since the space group is tetragonal, the $[0\bar{1}0]$ and $[100]$ directions are identical and we do not expect the degeneracy to be lifted.^{11,12} Cooling results in increased softening of the Σ_4 mode in both samples. For $x=0.6$, the phonon energy never reaches zero at the zone boundary as the crystal remains in the tetragonal phase. A summary of the temperature-dependent softening of the two modes at $(1.5\ 1.5\ 2)$ is shown in Fig. 4. Similar linear softening with tem-

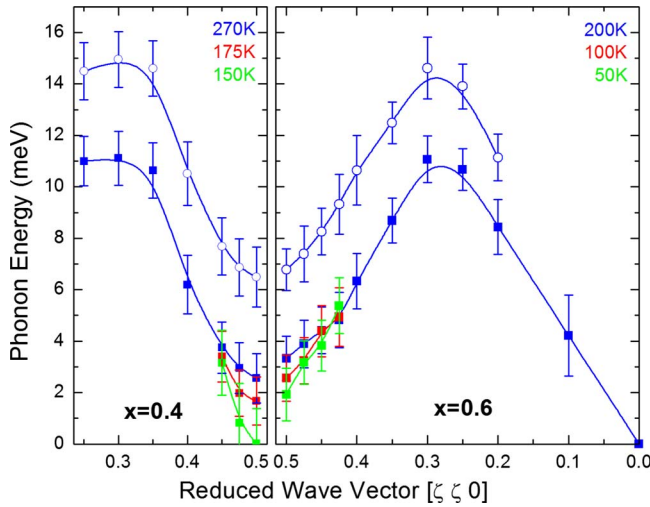


FIG. 3. (Color online) Dispersion of the Σ_4 (filled symbols) and anomalous (open symbols) phonon modes for both $x=0.4$ and $x=0.6$. The dispersion curves are plotted with the $I4/mmm$ Brillouin zone of the parent compound Sr_2RuO_4 . The Σ_4 mode shows typical soft-mode behavior and the anomalous mode mimics the Σ_4 dispersion. Lines are added as guides for the eyes.

perature is observed in both samples for both modes with the exception of a deviation from linearity for $x=0.4$ below 200 K as the lower branch softens to zero energy at $T \sim 150$ K. Note that while this mode softens completely, its corresponding anomalous mode never softens below 5 meV.

SrTiO_3 and La_2CuO_4 are classic examples where soft-phonon behavior drives structural instabilities.^{11,15} Displacive phase transitions are typically associated with a soft-phonon mode that freezes into a static lattice distortion at a critical temperature.¹⁶ For example, the energy of the Σ_4 tilt mode reduces to zero at the Brillouin-zone boundary in La_2CuO_4 at the HTT-LTO phase transition.¹¹ The Σ_4 transverse-acoustic phonon mode represents a rotation (in-

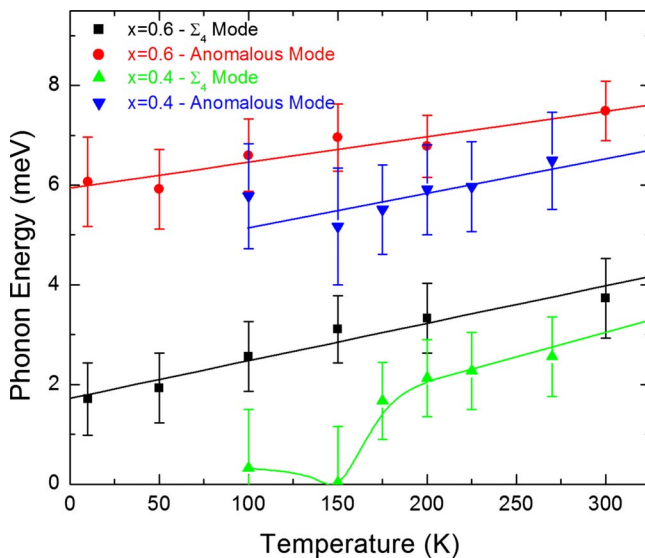


FIG. 4. (Color online) Zone-boundary softening for the Σ_4 and anomalous modes. The Σ_4 mode reaches zero energy as the phase boundary is crossed.

plane tilt) of the CuO_6 octahedron about an axis in the ab plane.¹⁷ Because $\text{Ca}_{2-x}\text{Sr}_x\text{RuO}_4$ has the same oxygen octahedron structure and also undergoes a HTT-LTO phase transition ($0.2 < x < 0.5$), one expects similar softening behavior in the CSRO family. However, there are significant differences in symmetry for the LSCO and CSRO systems. At higher values of $x \approx 1.5$, CSRO has already undergone a structural transition resulting from the freezing of a Σ_3 phonon mode with corresponding static rotation of the octahedra about the c axis.⁴ Thus, the HTT-LTO transition in CSRO (LSCO) is from space group $I4_1/acd$ to $Pbca$ ($I4/mmm$ to $Cmca$). One obvious consequence of the different space groups is that there is no change in the shape of the Brillouin zone during the HTT-LTO phase transition in CSRO. Despite this difference, the point-group symmetry for Ru is identical in both $I4/mmm$ and $I4_1/acd$ and, therefore, one does not expect any degeneracy lifting as a result of this difference.

Little is known about the tetragonal-to-tetragonal phase transition in CSRO that occurs at $x \approx 1.5$. The transition is from the space group $I4/mmm$ to $I4_1/acd$, caused by the rotation of the RuO_6 octahedra about the c axis. It is believed that the $x \approx 1.5$ structural transition in Sr_2RuO_4 results from the softening of the Σ_3 mode.¹² For $0.5 \leq x < 1.5$, a second-order structural phase transition into the $I4_1/acd$ phase is observed.^{4,10} Although the symmetry is $I4_1/acd$, disorder in the c -axis periodicity of the RuO_6 rotation is observed. Such disorder introduces stacking faults, resulting in a mixture of $I4_1/acd$ and $Acam$ symmetries as shown in Fig. 1. As x is decreased, the disorder in the c -axis periodicity is reduced and a more perfect $I4_1/acd$ phase is formed.^{4,10}

This anomalous mode was reported previously in the thesis of Friedt¹⁰ and tentatively attributed to interactions resulting from the different stacking periods of the tilt and rotational distortions combined with disorder in Ca/Sr mixing.¹⁰ The lack of anomalous phonon mode observations in other doped transition-metal oxides, such as the cuprates, and the static energy of the anomalous mode as the Σ_4 mode softens through the phase boundary suggest an alternate mechanism. We propose a simple model of intrinsic disorder within the $I4_1/acd$ symmetry to explain the anomalous mode. While the symmetry for $0.5 < x < 1.5$ is $I4_1/acd$, disorder along the c axis exists with a coherence length of approximately two unit cells observed for $x \sim 1.0$.¹⁰ It has also been observed that as more Ca is added to the system, a more perfect $I4_1/acd$ symmetry forms, resulting in fewer faults and an increased coherence length. It should be noted that long-range order exists within individual ab planes and it is only the c -axis disorder in the stacked layers of rotated RuO_6 that varies with x . Disorder in the c -axis octahedral rotation periodicity has also been observed in similar materials such as Sr_2IrO_4 and Sr_2RhO_4 .¹⁸ While interlayer coupling along the c axis is assumed weak as previous experiments suggest, it must occur for the well-coordinated RuO_6 rotations and tilts to exist along the c axis.^{4,12} The $I4_1/acd$ symmetry encodes four RuO_6 layers with a c -axis lattice parameter of ~ 25 Å. The structural frustration created from the rotational periodicity mismatch combined with the intrinsic stacking faults could lead to the formation of impurity domains of different symmetry ($Acam$) along the c axis and lift the phonon degeneracy. While locally the domains would appear to be

Acam, faults are isolated and random and the lack of *c*-axis correlation does not present a mixed-phase scenario nor would it appear in x-ray- or neutron-diffraction measurements. However, since the phonon propagates in the *ab* plane, local disorder could lift the degeneracy, allowing for spectral intensity in inelastic measurements. It has been observed in two-dimensional (2D) systems that disorder can alter phonon softening and prevent the freezing phonon from reaching zero energy at the phase transition.¹⁹ If the anomalous mode is due to disorder in the quasi-2D layered system, then one could expect that such a mode would soften to a finite temperature at the phase boundary as the Σ_4 mode reduces to zero energy.

In summary, inelastic-neutron-scattering experiments have been performed to measure the dispersion of the Σ_4 tilt mode phonon in $\text{Ca}_{1.4}\text{Sr}_{0.6}\text{RuO}_4$. The Σ_4 mode demonstrates typical soft-phonon behavior similar to La_2CuO_4 , but an anomalous phonon mode also appears. The anomalous mode mimics the Σ_4 dispersion except at the phase boundary

where the anomalous mode remains at finite energy, while the Σ_4 mode softens to zero energy, creating the orthorhombic phase. The anomalous mode is most likely due to disorder in the layered stacking sequence lifting the Σ_4 degeneracy. Further investigation is required to fully understand the role of defects and stacking faults in the CSRO family.

We thank I. A. Sergienko for helpful discussions. This work was supported by NSF Grants No. DMR-0346826, No. DMR-0353108, and No. DMR-0451163; DOE Grant No. DE-FG02-04ER46125; DOE DMS; and ORAU faculty summer research program. A portion of this research at Oak Ridge National Laboratory's High Flux Isotope Reactor was sponsored by the Scientific User Facilities Division, Office of Basic Energy Sciences, DOE. The work at Oak Ridge National Laboratory was supported through the Division of Materials Sciences and Engineering, Office of Basic Energy Sciences, DOE, under Contract No. DE-AC05-00OR22725.

*Present address: Stanford Synchrotron Radiation Lightsource, SLAC National Accelerator Laboratory, and Stanford Institute for Materials and Energy Sciences, Menlo Park, CA 94025.

¹Y. Maeno *et al.*, *Nature* (London) **372**, 532 (1994).

²Y. Maeno, T. M. Rice, and M. Sigrist, *Phys. Today* **54**(1), 42 (2001).

³S. Nakatsuji and Y. Maeno, *Phys. Rev. Lett.* **84**, 2666 (2000); *Phys. Rev. B* **62**, 6458 (2000).

⁴O. Friedt, M. Braden, G. Andre, P. Adelman, S. Nakatsuji, and Y. Maeno, *Phys. Rev. B* **63**, 174432 (2001).

⁵S. Nakatsuji, D. Hall, L. Balicas, Z. Fisk, K. Sugahara, M. Yoshioka, and Y. Maeno, *Phys. Rev. Lett.* **90**, 137202 (2003).

⁶B. Keimer, N. Belk, R. J. Birgeneau, A. Cassanho, C. Y. Chen, M. Greven, M. A. Kastner, A. Aharony, Y. Endoh, R. W. Erwin, and G. Shirane, *Phys. Rev. B* **46**, 14034 (1992).

⁷Z. Fang, K. Terakura, and N. Nagaosa, *New J. Phys.* **7**, 66 (2005).

⁸J. Baier *et al.*, *Physica B* **378-380**, 497 (2006).

⁹R. G. Moore *et al.*, *Science* **318**, 615 (2007); R. G. Moore, V. B. Nascimento, J. Zhang, J. Rundgren, R. Jin, D. Mandrus, and E. W. Plummer, *Phys. Rev. Lett.* **100**, 066102 (2008).

¹⁰O. Friedt, Ph.D. thesis, University of Paris, 2003.

¹¹R. J. Birgeneau, C. Y. Chen, D. R. Gabbe, H. P. Jenson, M. A. Kastner, C. J. Peters, P. J. Picone, T. Thio, T. R. Thurston, H. L. Tuller, J. D. Axe, P. Boni, and G. Shirane, *Phys. Rev. Lett.* **59**, 1329 (1987).

¹²M. Braden, W. Reichardt, S. Nishizaki, Y. Mori, and Y. Maeno, *Phys. Rev. B* **57**, 1236 (1998).

¹³E. D. Kolaczyk, *Astrophys. J.* **483**, 340 (1997).

¹⁴C. Charles *et al.*, *Surf. Interface Anal.* **36**, 49 (2004).

¹⁵G. Shirane, *Rev. Mod. Phys.* **46**, 437 (1974); J. F. Scott, *ibid.* **46**, 83 (1974).

¹⁶R. A. Cowley, *Adv. Phys.* **29**, 1 (1980).

¹⁷V. B. Grande, Hk. Müller-Buschbaum, and M. Schweizer, *Z. Anorg. Allg. Chem.* **428**, 120 (1977).

¹⁸M. K. Crawford, M. A. Subramanian, R. L. Harlow, J. A. Fernandez-Baca, Z. R. Wang, and D. C. Johnston, *Phys. Rev. B* **49**, 9198 (1994); M. A. Subramanian, *Physica C* **235-240**, 743 (1994).

¹⁹L. Petersen, Ismail, and E. W. Plummer, *Prog. Surf. Sci.* **71**, 1 (2002); R. Pérez, J. Ortega, and F. Flores, *Phys. Rev. Lett.* **86**, 4891 (2001); A. V. Melechko, M. V. Simkin, N. F. Samatova, J. Braun, and E. W. Plummer, *Phys. Rev. B* **64**, 235424 (2001).